The Astrophysical Journal, 308:213–224, 1986 September 1

THE BURSTING BEHAVIOR OF THE TRANSIENT X-RAY BURST SOURCE EXO 0748−676: A DEPENDENCE BETWEEN THE X-RAY BURST PROPERTIES AND THE STRENGTH OF THE PERSISTENT EMISSION

M. Gottwald,[1] F. Haberl,[1] A. N. Parmar,[1] and N. E. White[1]
Exosat Observatory, ESOC, Darmstadt, West Germany
Received 1985 October 16; accepted 1986 February 19

ABSTRACT

Between 1985 February 15 and July 19 *EXOSAT* made eight observations of the transient X-ray source EXO 0748−676. Within this time interval the persistent flux varied by a factor of 5 from a high to a low state and back to a high state. We observed 26 type I bursts, of which 22 were analyzed in detail. As the persistent flux decreased, the burst frequency increased and the burst shape changed from a "fast" to a "slow" profile. The ratio, α, of the total persistent energy before a burst to the total energy emitted in the burst varied between 20–30 and 60–300 and was correlated with the strength of the persistent flux. In addition, the apparent blackbody radius during the cooling tail was also correlated with the level of the persistent flux and varied from $\sim$4 to 9 km (for a fixed apparent temperature). At low persistent flux four sets of double bursts were recorded with a burst interval of 10–20 minutes. The apparent radii of these bursts were identical to their predecessors ($\sim$4 km). These variations in burst behavior are discussed in terms of accretion rate dependent changes in the thermonuclear flash process on the surface of a neutron star. We suggest that as the accretion rate decreases, the thermonuclear flash changes character from helium dominated to combined hydrogen/helium burning.

Subject headings: stars: individual — X-rays: binaries — X-rays: bursts

I. INTRODUCTION

Type I X-ray bursts show a great variety in their properties not only from source to source, but also in different bursts seen from an individual source. Burst intervals can vary from as short as 10 minutes up to several days. In addition the peak burst strength and its profile can show marked variations from one burst to the next. Detailed calculations have confirmed the early suggestion by Maraschi and Cavaliere (1977) and Woosley and Taam (1976) that the thermonuclear ignition of freshly accreted material on the surface of a neutron star provides a sound basis for understanding the global properties of X-ray burst sources (e.g., Joss 1977; Taam and Picklum 1978; Taam 1980; Fujimoto, Hanawa, and Miyaji 1981; Ayasli and Joss 1982). While these calculations have not attempted to reproduce in detail variable burst properties from a given burst source, they have indicated that variations in the mass accretion rate and the temperature of the neutron star core would give rise to changes in the burst properties.

The temperature of the neutron star core is important because the thermonuclear flashes are driven by a thermal instability. Any variation in the core temperature caused by heating from the flashes themselves will change the properties of subsequent bursts (Taam 1981). Variations in the accretion rate are also important in determining the temperature of the neutron star envelope and also the nature of the flash (Fujimoto, Hanawa, and Miyaji 1981). While the ignition of hydrogen is too slow to give the observed burst profiles, its mixture with helium can dramatically alter the properties of the helium flash by increasing the amount of nuclear energy available. If the hydrogen burns continuously, then its rate of burning is limited by the CNO cycle. Above accretion rates of $\sim 3 \times 10^{16}$–10^{17} g s^{-1} (depending on properties of the neutron star) hydrogen will not be completely burned and its addition to the helium flash will change the character of the burst by increasing the amount of nuclear energy available (Taam and Picklum 1979; Fujimoto, Hanawa, and Miyaji 1981). In addition it is possible that at low accretion rates ($< 3 \times 10^{15}$–2×10^{16} g s^{-1}) hydrogen burning may become intermittent resulting in hydrogen triggered helium flashes. In a regime between the two critical accretion rates the stable burning of hydrogen leads to helium flashes (Fujimoto, Hanawa, and Miyaji 1981). For high accretion rates in excess of 10^{18} g s^{-1}, the temperature of the envelope will rise to the point where helium burning becomes stable and the bursting activity ceases (Ayasli and Joss 1982).

These models suggest that changes in burst properties will be associated with changes in accretion rate, and there have been several efforts over the past 10 yr to search for intensity-dependent variations. The problem is deconvolving these effects from those caused by changes in the temperature of the neutron star core. Some results have indeed suggested that burst properties like the burst recurrence time or the burst shape may depend on the level of the persistent emission (e.g., Clark *et al.* 1977; Murakami *et al.* 1980*a*). In other instances, however, burst patterns change dramatically on a time scale of hours, sometimes with the bursting activity ceasing for several days, but with no obvious correlation with variations in the level of the persistent flux (Lewin *et al.* 1980).

Another puzzling result is that in a few instances a second X-ray burst has been seen from the same source about 10 minutes after its predecessor, far too soon for enough material to have accumulated to fuel a second thermonuclear flash (Murakami *et al.* 1980*b*). The second burst may be caused by partial burning of material on the neutron star surface, although no thermonuclear model constructed to date has predicted such an effect.

[1] Affiliated to Astrophysics Division, Space Science Department of ESA.

Observations have in the past been hampered by the fact that they utilized satellites that are in 100 minute low Earth orbits with the observation interrupted by passage through regions of high particle background and Earth occultations. This has usually made it impossible to determine α, the ratio of the energy emitted in the persistent emission before a burst to the energy emitted in the burst, for individual bursts because of possible "missed bursts" and gaps in the coverage of the history of the persistent emission. It has also made it difficult to identify recurring burst patterns and their relation to variations in the persistent emission.

The European Space Agency's orbiting observatory *EXOSAT* is the first X-ray astronomy mission with high sensitivity to be placed in a 90 hr orbit around Earth. This orbit allows continuous coverage of X-ray sources for up to 80 hr. In this paper we report a series of observations made by *EXOSAT* of the X-ray burst source EXO 0748−676. This transient X-ray source was discovered by *EXOSAT* in 1985 February and displays 8 minute eclipses with a period of 3.8 hr (Parmar *et al.* 1985). Over an interval of four months the persistent emission varied on a time scale of several weeks by a factor of 5. In this paper we report a systematic study of the properties of 22 type I bursts recorded from this source and their relation to the level of the underlying persistent emission.

II. OBSERVATIONS

The details of the observations are given in Parmar *et al.* (1986, hereafter Paper I). Briefly, there were eight pointed observations between 1985 February 15 and 1985 July 19 whose duration lasted between 6 and 24 hr. The data to be presented here come from the argon layer of the Medium Energy experiment (ME; Turner, Smith, and Zimmermann 1981) in the energy range 1–15 kev. Pulse height analyzer data were obtained in 128 channels with a time resolution of 1 s in all but two observations; in these cases the resolution was 0.375 s for one observation and 2 s for the other.

III. RESULTS

a) Burst Frequency

The time-averaged persistent flux as calculated from periods around bursts (excluding bursts, dips, and eclipses; cf. Paper I) measured during each observation is summarized in Table 1. Whenever flux values or luminosities are given in this paper they refer to the energy band 0.1–20 keV (this is different from the convention used in Paper I). This energy range was chosen

TABLE 1

LONG-TERM BEHAVIOR OF PERSISTENT FLUX f_p AND BURST OCCURRENCE

Observation Date[a] (1985)	Exposure Time (10^4 s)	f_p (0.1–20 keV) (10^{-10} ergs cm^{-2} s^{-1})	N[b]
Feb 15 (46)	8.4	10.5–13.2	4
Feb 18/19 (49/50)	6.2	8.1–12.5	2
Feb 26 (57)	6.1[c]	7.4	5
Mar 10 (69)	3.2	4.0	4
Mar 28/29 (87/88)	3.6	3.8	6
Apr 8/9 (98/99)	2.8	3.0	4
Jun 1 (152)	4.5	17.9	1
Jul 19 (200)	2.2	13.5	0

[a] Number in parentheses is the day number of 1985.

[b] Number of bursts.

[c] Because of offset pointing for the first 3.1×10^4 s, only bursts from the final 3×10^4 s were analyzed in detail.

to obtain better estimates of the total flux in each burst and the total energy in the persistent emission. Data from the Low Energy Telescope (LE; de Korte *et al.* 1981) were included in the fits to the spectra of the persistent emission. In all eight observations from Table 1 the spectral model assumed in Paper I was consistent with the combined data from ME and LE. The source declined over an interval of 2 months from an initial value of $\sim 12 \times 10^{-10}$ ergs cm^{-2} s^{-1} to 3×10^{-10} ergs cm^{-2} s^{-1}. This trend was reversed in the final two observations, with the average source flux increasing to its brightest recorded level of $\sim 18 \times 10^{-10}$ ergs cm^{-2} s^{-1}. Within each observation the flux varied by at most 30%, and by $<10\%$ between bursts.

Figure 1 shows three representative light curves taken when the persistent flux was at 10×10^{-10} ergs cm^{-2} s^{-1} on February 18/19, at 7.4×10^{-10} ergs cm^{-2} s^{-1} on February 26, and at 3×10^{-10} ergs cm^{-2} s^{-1} on April 8/9. X-ray bursts are visible as narrow spikes. The eclipses and dips in the light curves are discussed in Paper I. During the February 18/19 observation there is a long interval of at least 15 hr where no bursts were seen (gaps in the ME data were checked for bursts from an analysis of the ME housekeeping data and the simultaneously recorded data from the Gas Scintillation Proportional Counter [GSPC; Peacock *et al.* 1981]). This interval is terminated by a relatively large burst that is followed 2.5 hr later by a smaller burst. Figure 1 in Paper I shows the light curve obtained on February 15, when the persistent emission was also at $\sim 10 \times 10^{-10}$ ergs cm^{-2} s^{-1}. This reveals a similar pattern with three small bursts separated by ~ 3 hr, followed by a 16 hr interval with no bursts, terminated by a large burst. During observations when the persistent emission was at a level of $< 5 \times 10^{-10}$ ergs cm^{-2} s^{-1}, there were several instances of bursts separated by only $\sim$10–20 minutes (cf. Fig. 4); these are similar to the multiple burst events reported by Murakami *et al.* (1980*b*, see also Lewin *et al.* 1976). If these "double bursts" are counted as one complete event, then the typical separation between events is of order 2–3 hr with no extended intervals of burst inactivity.

The longest observation times (17 hr and 24 hr) were obtained for the first two observations when the source was at a level of $> 7.5 \times 10^{-10}$ ergs cm^{-2} s^{-1}. A total of seven bursts were observed with intervals between 9,000 and 57,000 s which gives an average burst frequency of 0.12 burst hr^{-1} (the upper limit is 0.25 burst hr^{-1} provided one burst was missed just at the beginning and end of the observation). For an intermediate persistent flux level of 5×10^{-10} ergs cm^{-2} s^{-1} $< f_p < 7.5 \times 10^{-10}$ ergs cm^{-2} s^{-1} (transition from high to low state), the burst frequency increased to 0.30 burst hr^{-1} with an upper limit of 0.41. The typical exposure times obtained in later observations when the source was below 5×10^{-10} ergs cm^{-2} s^{-1} were of 7–8 hr length. If the double bursts are treated as single events then the average burst rate derived for these observations is 0.40 (<0.64). When all individual bursts are included this rate increases to 0.56 (<0.80). It would be possible that the difference in burst rate is only caused by the shorter observation lengths used when the source was at low levels. The fact that we observed that source 3 times in a low state without recording long recurrence times between bursts and then observed it at high persistent flux with similar exposure length (June 1, July 19) and again recorded long burst intervals argues against this being the case.

While the continuous coverage afforded by the *EXOSAT* Observatory allows individual burst intervals to be measured,

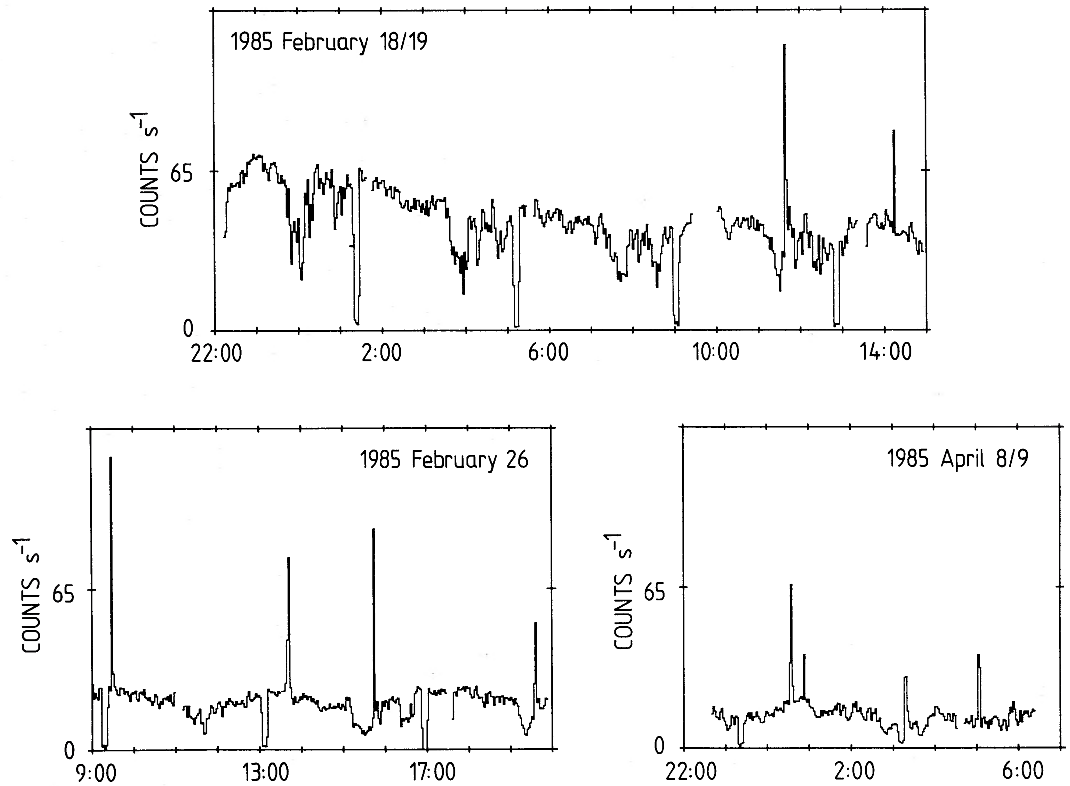

FIG. 1.—Three representative light curves of EXO 0748−676. During the period from February 18/19 to April 8/9 the source went from a high to a low state. For the observation on February 26 the light curve between UT 09:00 and UT 11:00 is corrected for offset pointing, but the burst at UT 09:28 was discarded from the burst spectral analysis.

there remains the possibility with this particular source that a burst may be missed because it occurs during the 8 minute eclipse by the companion star. In Paper I it was shown that there is residual emission during the eclipse at a level of 4% of the uneclipsed level. This emission is caused by X-rays scattered around the companion by a corona or wind above the accretion disk and also from scattering by interstellar dust causing a halo around the source (Paper I). Above 2 keV scattering by an accretion disk corona dominates such that any burst that occurs during an eclipse should still be visible during the eclipse at a low level. We have searched each eclipse for such events, and in one case there is evidence for a burst. This forms part of a double burst and is discussed in more detail below.

We conclude that the burst rate is strongly anticorrelated with the level of the persistent emission, and that at higher flux levels the burst pattern becomes irregular. In addition double bursts, i.e., those where a second burst occurred within 10–20 minutes of a previous event, were seen only when the persistent flux was low. The occurrence rate of these events when the persistent flux was below 5×10^{-10} ergs cm^{-2} s^{-1} was high at 0.16 double bursts hr^{-1}. If these events were uniformly distributed at all persistent flux levels, then 12 of these events should have been detected when the source was brighter than 5×10^{-10} ergs cm^{-2} s^{-1}.

b) *Burst Properties*

In Figure 2 we show the dependence of the peak burst count rate (C_p), the total number of counts (C_t) in each burst and the effective burst duration, defined by the ratio C_t/C_p on the level of the persistent count rate (all count rates are corrected for sampling dead time in the on-board computer). The double bursts are indicated by open circles. For single bursts the peak count rate increases by a factor of 10 as the persistent flux increases in the same sense by a factor of 5. The total count rate in each burst, however, does not strongly depend on the persistent level. This means that the effective burst duration is strongly anticorrelated with persistent emission, i.e., the bursts at low persistent flux level last longer. We refer to those bursts that have a duration <16 s as "fast" and those longer than this as "slow." No difference in rise time (time from burst onset to burst peak) exists between slow and fast bursts with an effective duration >8 s. Both burst modes have $t_{\rm rise} \sim 6$ s. The three strong bursts occurring after long wait times (Table 2, duration <8 s) exhibit very short rise times of <1–2 s.

The total count rate in the second burst of a double burst was always a factor of 3 less than that in its predecessor. In addition the total counts in the first burst that forms part of a pair was the same as that in surrounding single events. In contrast the second burst in the double has a much shorter duration, similar to that of bursts seen when the persistent flux was high.

Figure 3 displays three representative burst profiles with durations of 6, 15, and 41 s. In addition in Figure 4 the three double bursts seen in our observations are shown for comparison. The burst intervals in these cases are 10, 15, and 19 minutes. In Figure 5 the light curve of the March 28 observation is shown. The double burst given in Figure 4 can be seen around UT 01:00. Just after an eclipse at UT 19:45 a small burst occurred that is very similar to the second burst of the double seen 5 hr later. Expanded views of the eclipse and the burst that follows (Figs. 5*b* and 5*c*) illustrate that shortly after

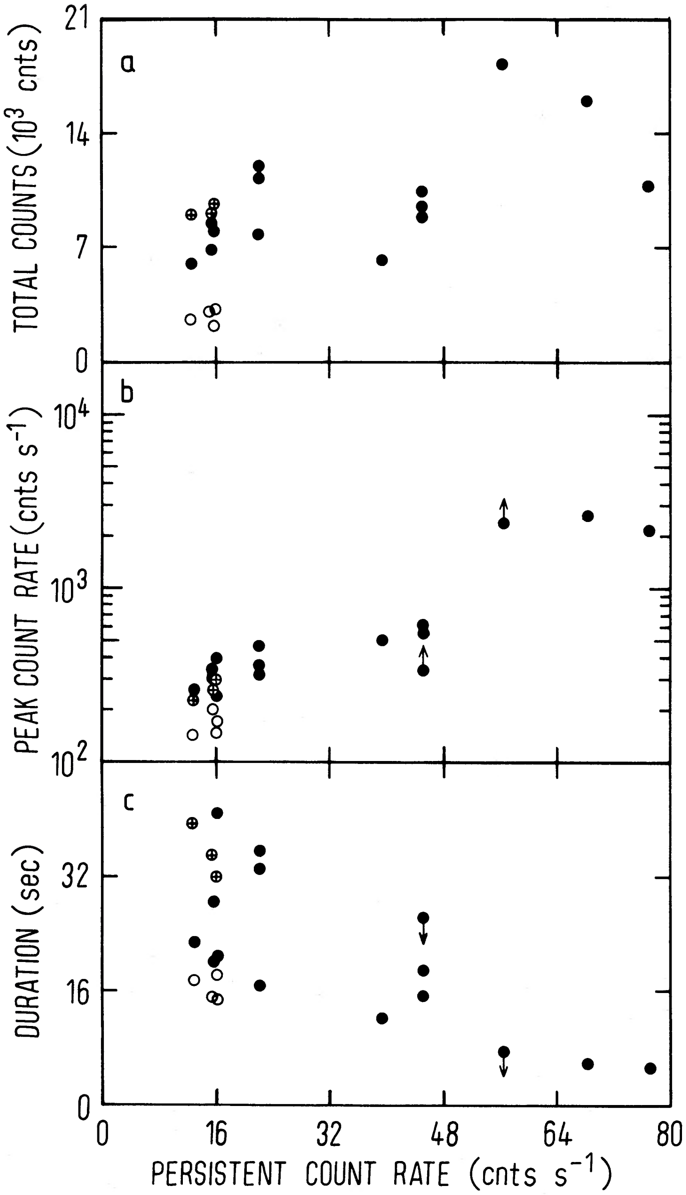

FIG. 2.—Total number of ME counts in a burst (*a*), peak burst count rate (*b*), and burst duration (*c*) for 22 bursts of EXO 0748−676 as a function of the persistent count rate (*filled circles:* single bursts; *crossed circles:* first bursts in double bursts; *open circles:* second bursts in double bursts).

the eclipse ingress, a rise in counts almost up to the preeclipse level is evident. This would appear to be the first burst of a double burst. The expected total number of counts in such a burst (we use total number rather than peak count rates to avoid any problems with smearing by light travel time effects) should be ∼9000 counts (Fig. 2). For the observed total number of counts in the burst of ∼360 counts, this indicates that ∼4% of the emission was scattered around the companion, consistent with the estimates given in Paper I.

IV. SPECTRAL PROPERTIES

The time evolution of the spectral properties of each burst was studied by obtaining dead-time–corrected pulse height spectra with a time resolution of 1 s for the brightest bursts, and 2–3 s for the fainter ones. The time intervals used were optimized to avoid smearing out any spectral variations across the peak of the bursts. As the burst decayed the accumulation time was increased to 5–10 s. The background was obtained from intervals preceding and following the burst and included the persistent emission from the source. Because the underlying source flux was quite variable, care was taken in each case to ensure that the subtraction was correct. One burst that occurred in the middle of a very deep dip, the one that occurred during an eclipse and two for which the spacecraft pointing was not stable were discarded. A total of 22 bursts were considered acceptable.

Blackbody fits were made to the data with the normalization I_0, color temperature kT_c and equivalent low-energy absorption N_H allowed to be free parameters. We refer to this as a "color" temperature because radiative transfer effects in the neutron star atmosphere will distort the blackbody spectrum.

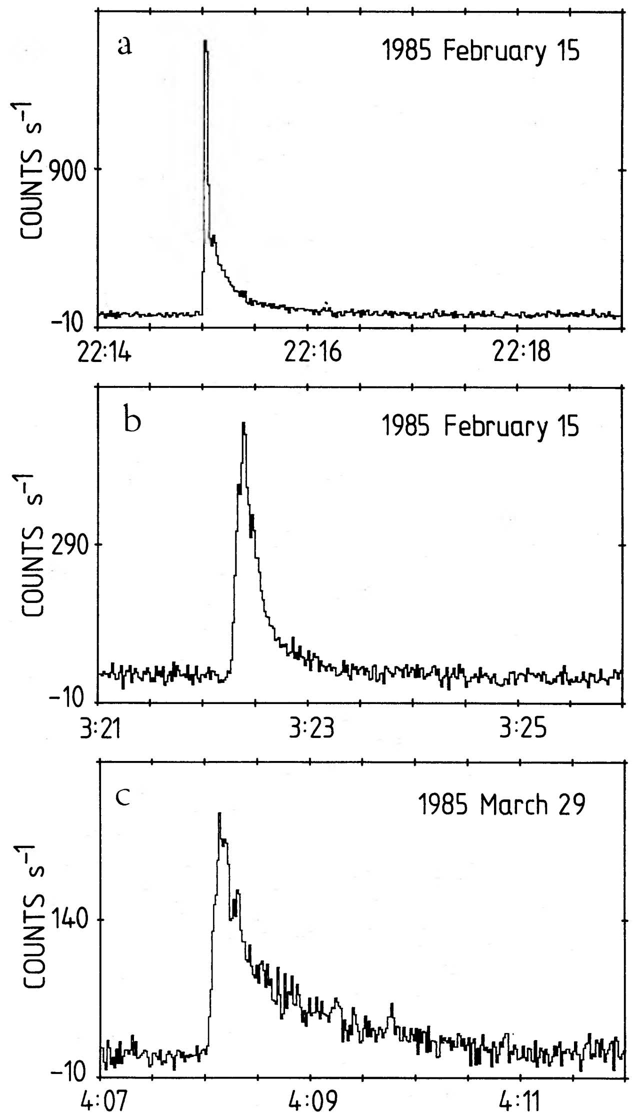

FIG. 3.—Light curves of representative "fast" (*a*) and (*b*) and "slow" (*c*) bursts in the energy range 1.5–15 keV (time resolution 1 s; horizontal: UT in hh:mm). Burst (*a*) showed radius expansion in its initial phase. The light curves are not dead-time corrected. Dead-time correction factors for the bursts peaks are 1.56 (*a*), 1.23 (*b*), and 1.13 (*c*).

TABLE 2

ANALYZED BURSTS

Burst Onset (1985 day/UT)	Δt_w[a] (s)	f_{peak} (0.1–20 keV) (10^{-9} ergs cm^{-2} s^{-1})	f_{total} (0.1–20 keV) (10^{-7} ergs cm^{-2})	α
46/00:48:35.........	>2480	>6.23	0.90 ± 0.14	>29
46/03:22:15.........	9220	12.50 ± 1.68	1.46 ± 0.47	59
46/06:16:26.........	10451	10.40 ± 1.70	1.59 ± 0.10	69
46/22:14:59.........	57513	37.10 ± 3.47	2.50 ± 0.16	304
50/11:38:28.........	>48090	>32.30	2.85 ± 0.12	>210
50/14:14:18.........	9350	9.04 ± 1.36	0.96 ± 0.09	79
57/13:40:41.........	15160	4.71 ± 1.53	1.48 ± 0.10	75
57/15:43:26.........	7365	5.63 ± 0.87	1.67 ± 0.07	32
57/19:34:41.........	13875	9.96 ± 2.13	1.41 ± 0.11	72
69/09:21:40.........	>6100	4.77 ± 1.03	1.41 ± 0.08	>17
69/09:32:07.........	627	3.21 ± 0.48	0.46 ± 0.05	5
69/12:45:23.........	11596	5.68 ± 1.07	1.79 ± 0.10	26
69/15:08:34.........	8591	4.72 ± 1.22	1.15 ± 0.09	29
87/19:50:55.........	780	3.67 ± 1.43	0.58 ± 0.09	5
87/22:33:39.........	9764	8.95 ± 1.70	1.43 ± 0.09	26
88/01:02:43.........	8944	5.82 ± 1.05	1.56 ± 0.09	22
88/01:18:23.........	940	2.34 ± 0.84	0.38 ± 0.05	9
88/04:08:02.........	10179	5.17 ± 1.35	1.72 ± 0.13	22
99/00:33:48.........	>6800	5.25 ± 0.98	1.40 ± 0.09	>14
99/00:52:52.........	1144	3.10 ± 0.89	0.39 ± 0.06	9
99/05:03:37.........	6380	4.82 ± 1.16	1.04 ± 0.08	18
152/08:58:14.........	>18734	28.80 ± 3.28	1.69 ± 0.15	>198

[a] Burst recurrence time.

This will cause the measured temperature to be an overestimate of the true value and any radius for a spherical emitter derived using that temperature an underestimate (London, Taam, and Howard 1984; Ebisuzaki and Nomoto 1985). These effects become most acute at higher temperatures and will cause an anticorrelation between apparent temperature and radius, with the magnitude of the effect depending on the composition of the neutron star envelope (Matsuoka 1985 and references therein).

In all cases a blackbody spectrum provided an acceptable description of the data with the average reduced χ^2_r between 1.1 and 1.5. No narrow spectral features were visible in the ME spectra (also not in the GSPC spectra, although these data were of much lower quality). Quoted errors are 1 σ uncertainties. The best-fitting column densities were all less than 1.4×10^{22} H cm^{-2}, consistent with that obtained for the persistent emission in Paper I (0.5×10^{22} H cm^{-2}). The best-fitting parameters were used to derive the flux at the source in the 0.1–20 keV band, from which the luminosity L_a, and apparent blackbody radii R_a, were obtained for a spherical emitter at an arbitrarily assumed distance of 10 kpc (with no correction for relativistic effects).

Figure 6 shows the evolution of kT_c and L_a through the first 60 s of each burst, except for the second in a double burst where only 30 s after the onset could be followed. The bursts have been divided into two groups depending on whether the level of the persistent emission was above 7.5×10^{-10} ergs cm^{-2} s^{-1} or below 5×10^{-10} ergs cm^{-2} s^{-1} and are plotted on the left- and right-hand sides of Figure 6. The double bursts are indicated in Figures 6*c* and 6*d* by open and crossed circles. Three of the largest bursts, those following a long wait time of >5 hr, showed luminosities in excess of the Eddington limit for the assumed distance of 10 kpc; these have been indicated in Figures 6*a* and 6*b* as open circles.

The evolution of kT_c during the burst decay shows a pronounced difference for bursts emitted at different persistent flux levels. While the peak color temperature is approximately the same in all cases at ~2.2 keV, bursts emitted when the persistent flux is higher apparently cool much faster. The first burst of a double burst is indistinguishable on this diagram from other bursts recorded at the same persistent flux level. The second burst in a double is, however, different with a lower peak temperature of 1.9–2.0 keV and a more rapid decay.

In Figure 7 the apparent radius and luminosity are shown as a function of temperature depending on the level of the persistent emission. On the right-hand side (*c*, *d*; low state), crossed and open circles again denote the first and second bursts in a double. The apparent temperatures during the super-Eddington portion of the burst (*a*, *b*) are low such that the apparent radii increases to 25–30 km. This radius expansion during the early part of the strongest bursts goes off scale and is indicated by arrows; during the decay portion of these bursts the properties are identical to other less luminous bursts. Similar radius expansion in the initial phase of energetic bursts also has been reported for MXB 1728−34 (Basinska *et al.* 1984), MXB 1636−53 (Ohashi *et al.* 1982) and 4U 1820−30 (Vacca, Lewin, and van Paradijs 1985). When the persistent flux is low and the bursts slow, the apparent radius is ~4.4 km with no strong dependence on temperature. When the persistent flux is high and the bursts fast, there is a strong anticorrelation of the apparent burst radius from 7 to 11 km as the temperature decreases from 2.3 to 1.2 keV. In particular the radius of a burst at a given temperature is a factor of 2 lower when the persistent flux is lower (and the bursts are slow). For $kT_c = 1.6$ keV the corresponding radii are 8.7 ± 0.5 km and 4.4 ± 0.5 km at flux levels above 7.5×10^{-10} ergs cm^{-2} s^{-1} and below 5×10^{-10} ergs cm^{-2} s^{-1}.

The bursts emitted during a persistent flux level of 5×10^{-10} ergs cm^{-2} s^{-1} $< f_p < 7.5 \times 10^{-10}$ ergs cm^{-2} s^{-1} are not included in Figures 6 and 7. This flux level is close to the transition of the source from the high to the low state, and the burst properties therefore tend to lie at the limits of the values characteristic for the "fast" bursts (see below, Figs. 8 and 9).

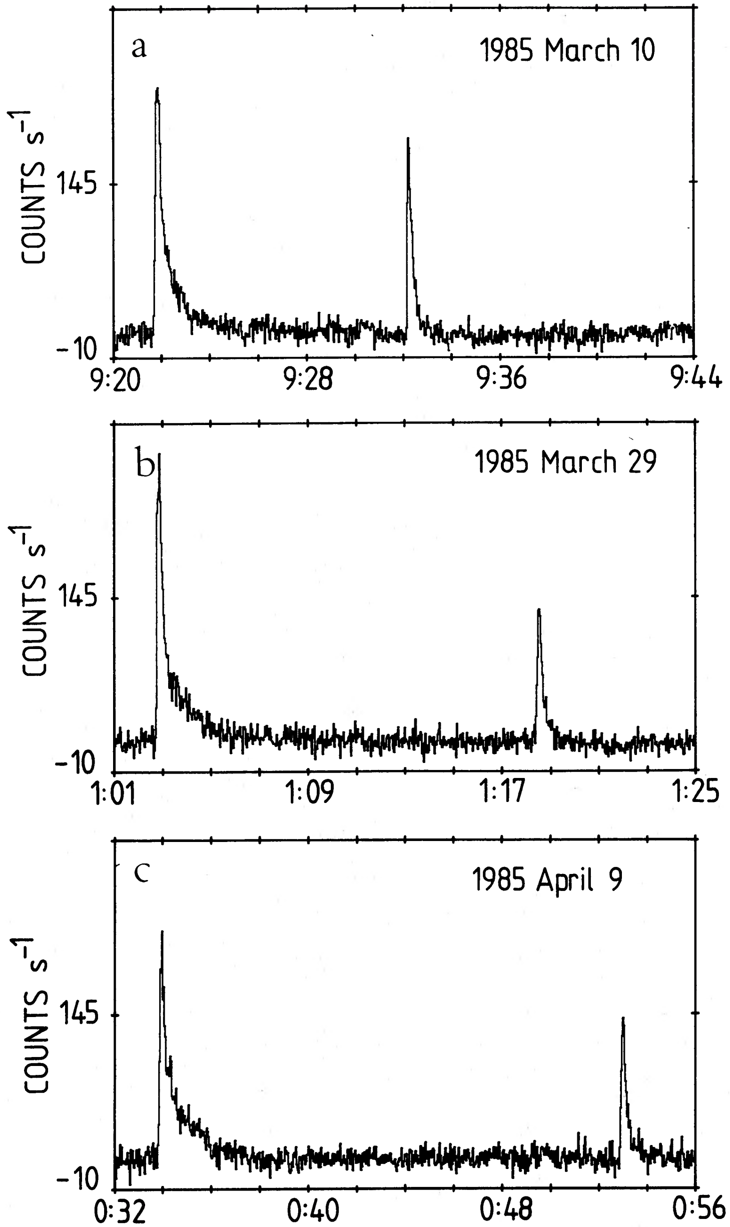

FIG. 4

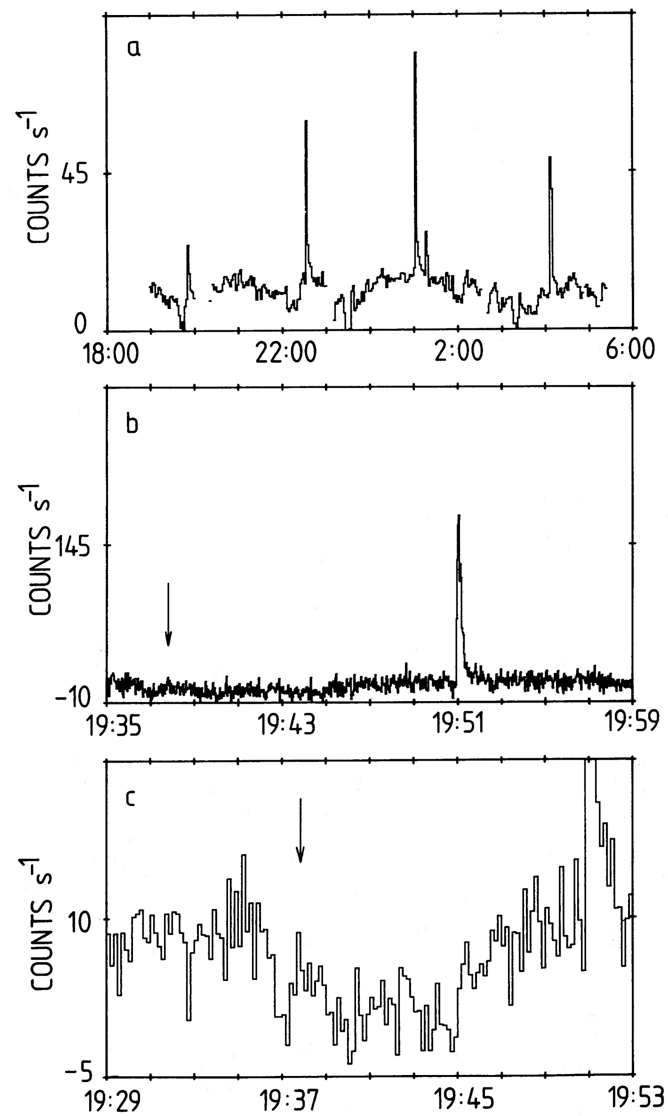

FIG. 5

FIG. 4.—Three double bursts from EXO 0748 − 676 (1.5–15 keV). Time resolution is 2 s with horizontal axis as in Fig. 3. The light curves are not dead-time corrected (correction factors for the burst peaks ∼ 1.13).

FIG. 5.—Detection of a partially eclipsed double burst on March 28. Time resolution is 120 s (*a*), 2 s (*b*), 10 s (*c*). Energy range and horizontal axis as in Fig. 3. The arrow indicates the time of the first burst. The eclipse lasts from UT ∼ 19:36:40 to 19:45:00 (light curves are not dead-time corrected).

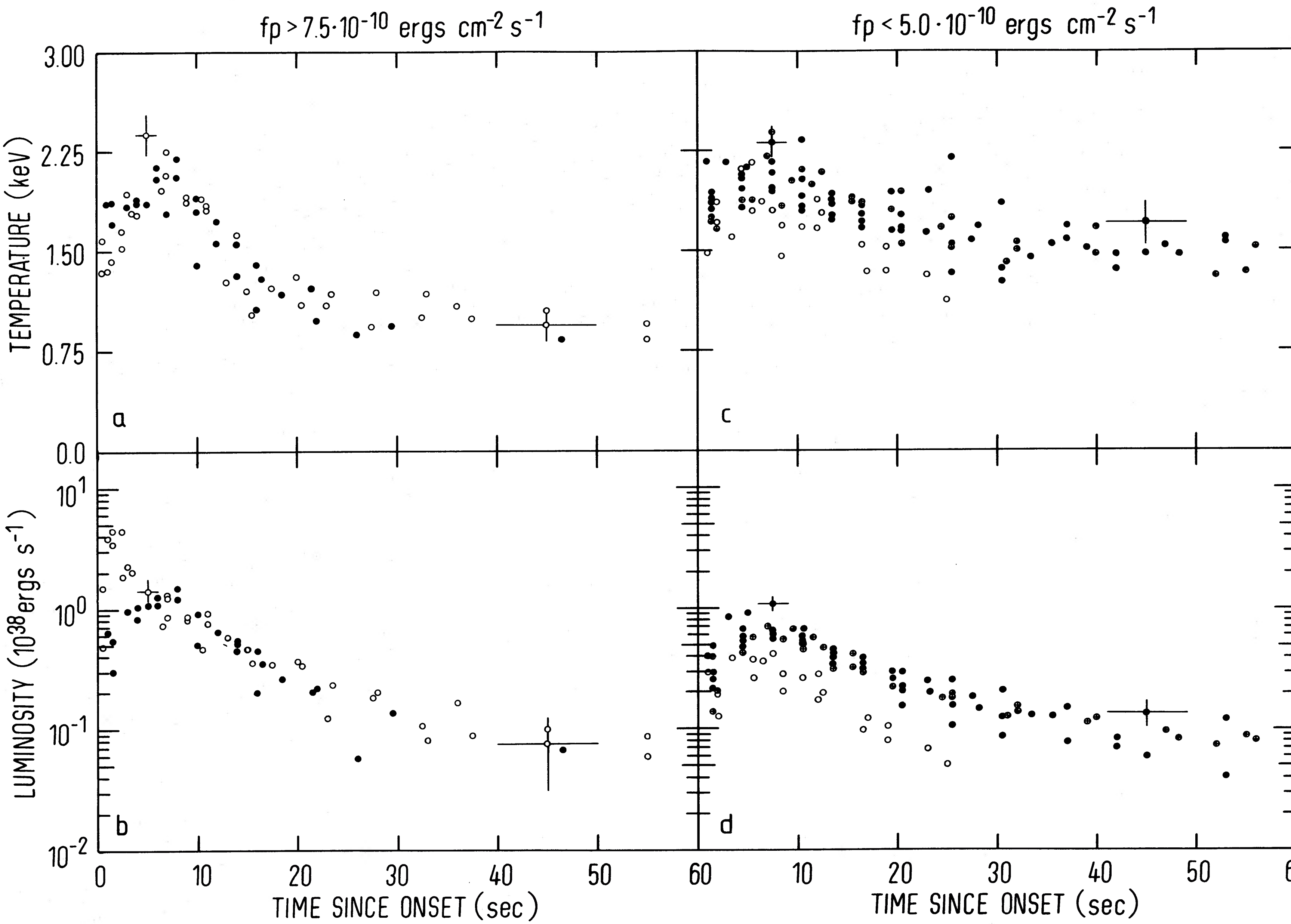

FIG. 6.—Spectral evolution for bursts from the high (*a*) and (*b*) and low (*c*) and (*d*) transient state in the first 60 s since the onset of the burst. High state is defined for persistent flux $f_p > 7.5 \times 10^{-10}$ ergs cm^{-2} s^{-1}, low state for $f_p < 5 \times 10^{-10}$ ergs cm^{-2} s^{-1} (0.1–20 keV). The luminosities in the lower panels are calculated from the blackbody-fit temperatures kT_c for an energy range 0.1–20 keV with an assumed distance of 10 kpc (1 σ statistical error bars are shown). In (*a*) and (*b*) open circles represent bursts with initial radius expansion, and filled circles, bursts without radius expansion. On the left side (*c*) and (*d*) filled circles indicate single bursts, crossed circles, first bursts in double bursts, and open circles, second bursts in double bursts.

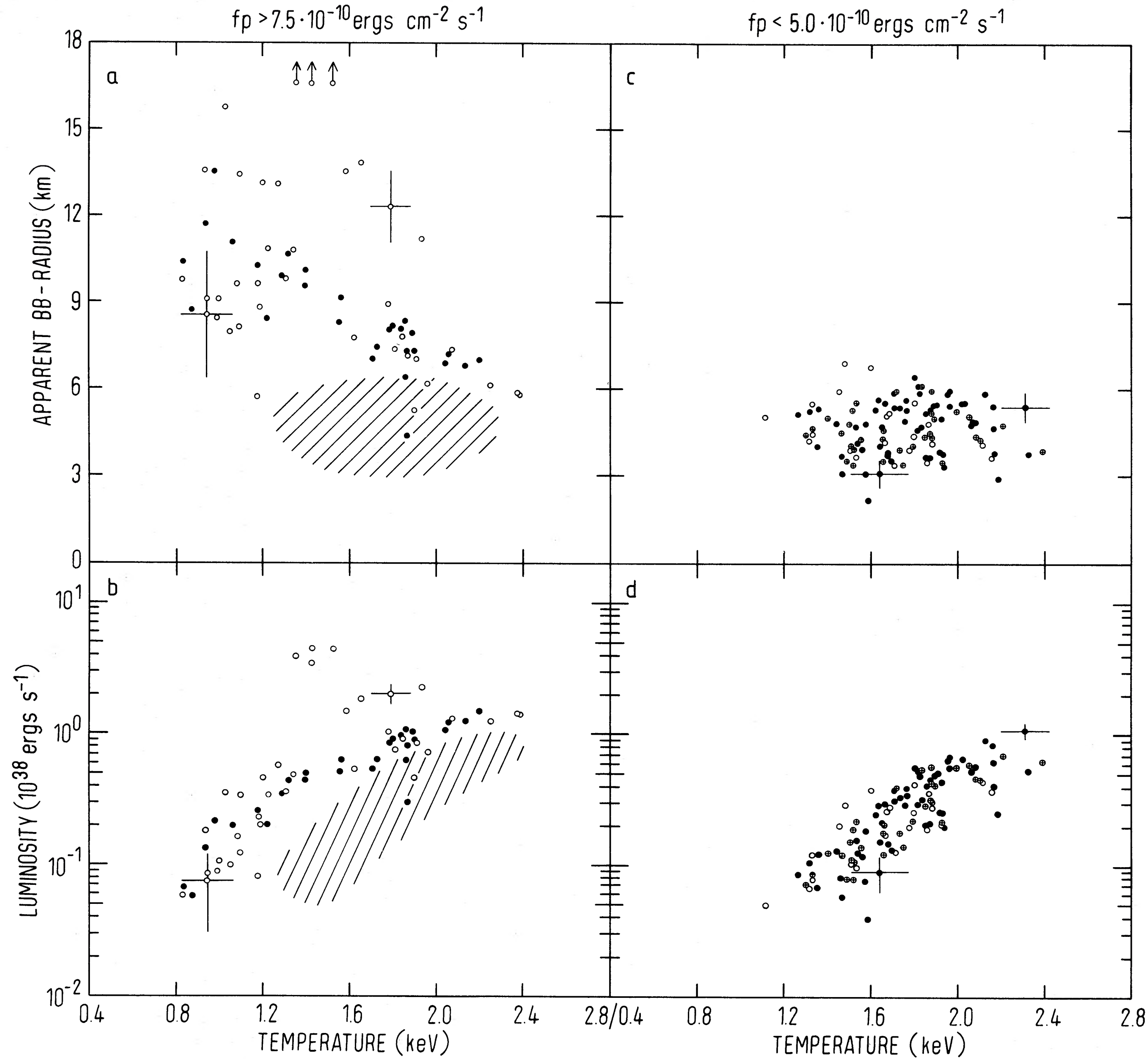

FIG. 7.—Variation of apparent bb-radius and luminosity (0.1–20 keV, distance 10 kpc) with temperature kT_c for bursts from the high (*a*) and (*b*) and low (*c*) and (*d*) transient state. In (*a*) three radii from the expansion phase (maximum $R_a \approx 30$ km) are plotted as lower limits. An anticorrelation between T_c and R_a is seen for bursts in (*a*) but not in (*c*). The lower panels show the different tracks in the kT_c/L_a diagram for the different burst modes. Hatched areas in (*a*) and (*b*) indicate the mean location of data points in (*c*) and (*d*). The symbols are the same as in Fig. 6. The level of persistent emission is given on top of the panels.

V. OVERALL CORRELATIONS

The value of α was computed for each burst. In Figure 8*a* we plot this as a function of the time-averaged value of the persistent flux. There is a good correlation between the two with α increasing from 20–30 to 60–300 as the persistent flux increases by a factor of 5. We also show in Figure 8*b* the apparent blackbody radius measured during the decaying phase of the burst as a function of luminosity. The strong correlation between apparent blackbody radius and the level of the persistent flux noted earlier is again evident. It is worth noting that these diagrams include one burst observed when the source had returned to its high state in June; there is no evidence that the correlation of the burst properties with intensity had changed after the prolonged interval at a lower flux level.

The α value for the first burst of a double (*filled circles*) is similar to that of single bursts seen at a similar flux level. The α derived for the second burst of a double is, as would be expected, very low with values ranging between 5 and 9 (*open circles*). The apparent blackbody radii are, however, identical to those obtained during the other normal bursts seen at the same persistent flux level; this includes both the first burst in a double and other bursts in the same sequence.

In Figure 9 the total flux in a burst is plotted as a function of

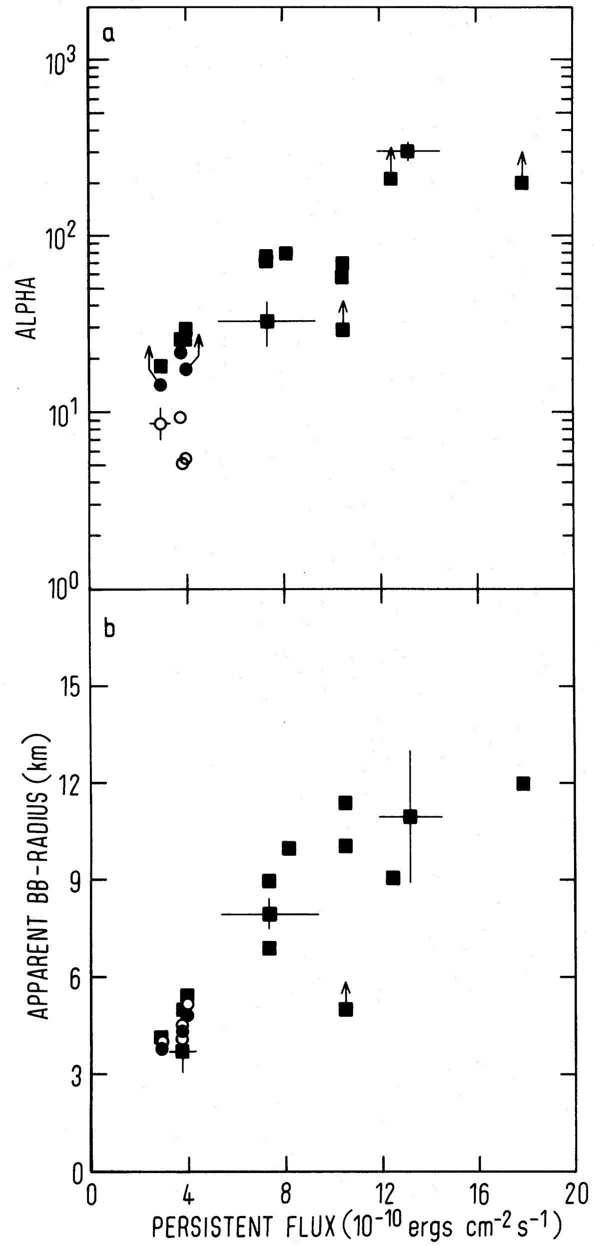

FIG. 8.—Apparent radius (*b*) and α (*a*) as a function of persistent flux. The radius is calculated as the average value in the burst tails. Squares denote single bursts, filled circles, first bursts in double bursts, and open circles, second bursts in double bursts.

the peak burst flux. When the persistent flux is high and the bursts "fast" (*squares*), the most energetic bursts tend to have the highest peak fluxes. The brightest bursts ($f_{\mathrm{peak}} > 2 \times 10^{-8}$ ergs cm^{-2} s^{-1}) also are the ones that show evidence for radius expansion. Bursts from the "slow" mode exhibit lower peak fluxes ($<0.8 \times 10^{-8}$ ergs cm^{-2} s^{-1}) but typically have similar total energy (*triangles* and *filled circles*). The second bursts in the double bursts show peak fluxes and total fluxes lower than that of the preceding bursts. The reduction in total flux is by a factor of 0.33 (March 10), 0.24 (March 29), and 0.28 (April 9).

The bursts with the highest peak and integrated fluxes always occurred after the longest waiting times (typically 50,000 s). For the remaining bursts the time elapsed since the previous bursts was usually between 7500 and 12,500 s. The total flux in a burst, f_{total}, is plotted in Figure 10 as a function of the average persistent flux multiplied by the wait time until that burst $f_p \times \Delta t_w$ ($\sim$ mass accumulation). Bursts recorded at higher flux levels ($>5 \times 10^{-10}$ ergs cm^{-2} s^{-1}) are denoted by squares and those at lower levels by triangles (single bursts) and circles (double bursts). If the energy in a burst were simply proportional to the amount of freshly accreted material since the last burst, then these points would lie along a line of constant α. The variations in α resulting from its correlation with the level of the persistent flux causes the points to lie away from such a relation. However, the subset of bursts observed at a high persistent flux level (where a large variation in burst intervals is seen) also do not lie on lines of constant α. While bursts that occur after a long wait have an α of typically > 200, for those with short wait times the derived value of α is 70. This trend can be expressed as $f_{\mathrm{total}} \approx (f_p \times \Delta t_w)^\gamma$ with $\gamma \approx 0.3$, i.e., the total energy in a burst does not depend linearly on the amount of fuel accumulated since the previous event for the subset of bursts observed at a high persistent flux level.

VI. DISCUSSION

These results can be summarized as follows:

1. The value of α is correlated with the level of the persistent flux and increases from $\sim$20–30 at low persistent flux levels ($<5 \times 10^{-10}$ ergs cm^{-2} s^{-1}) to 60–300 at higher values. This corresponds to an increase in the luminosity of the persistent emission from 3.6×10^{36} ergs s^{-1} to 2.2×10^{37} ergs s^{-1} for a source distance of 10 kpc.

2. The blackbody radius for a spherical emitter at 10 kpc measured during the decay of the bursts is, for a particular

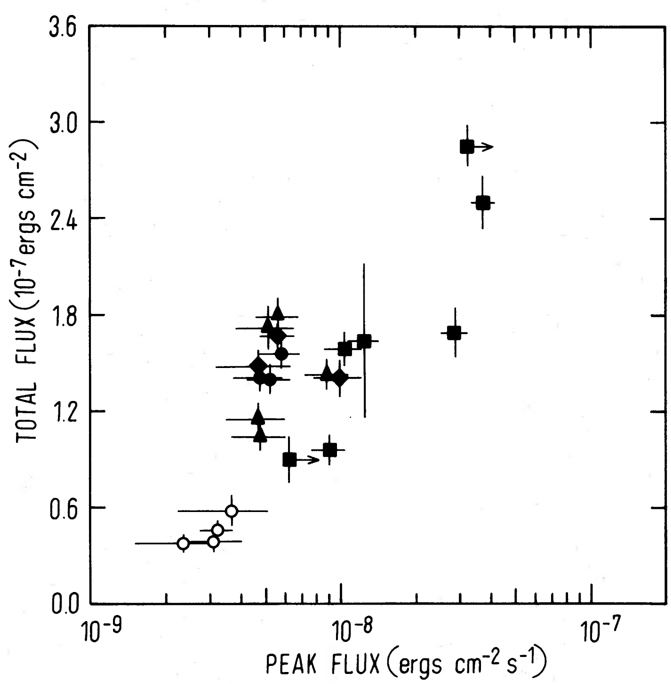

FIG. 9.—Relation between peak and total flux (0.1–20 keV) in the bursts of EXO 0748−676. The separation into two groups corresponds to the occurrence of different burst modes. Squares stand for bursts emitted at $f_p > 7.5 \times 10^{-10}$ ergs cm^{-2} s^{-1}, diamonds for $5 \times 10^{-10} < f_p < 7.5 \times 10^{-10}$ ergs cm^{-2} s^{-1} (transition from low to high state), triangles for $f_p < 5 \times 10^{-10}$ ergs cm^{-2} s^{-1}, filled circles for first bursts in double bursts, and open circles for second bursts in double bursts.

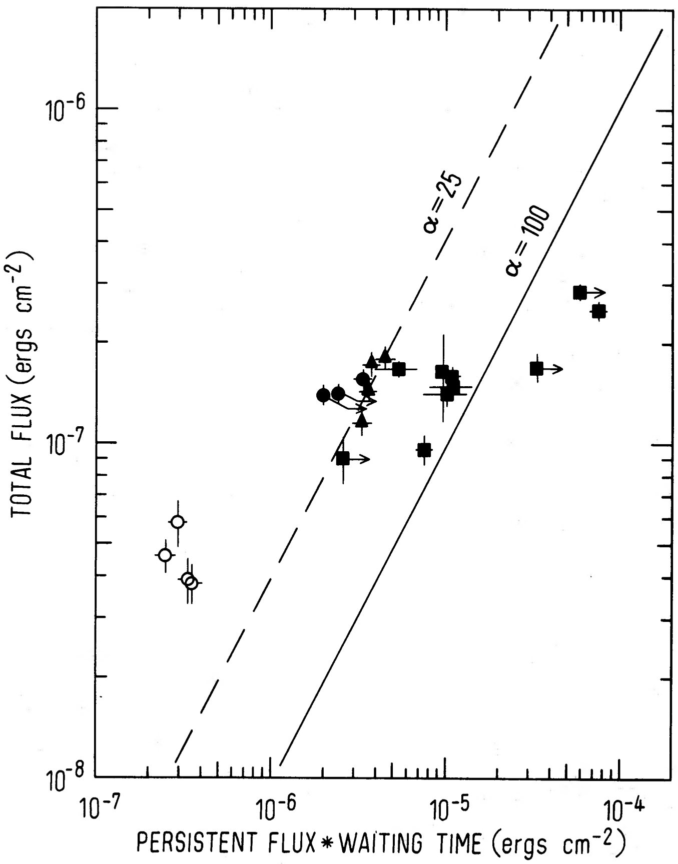

FIG. 10.—Total burst flux (0.1–20 keV) as a function of persistent flux times wait time ($\sim$ mass accumulation). Bursts emitted with identical α lie on straight lines. Squares denote bursts from the high transient state ($f_p > 5 \times 10^{-10}$ ergs cm^{-2} s^{-1}), triangles from the low state ($f_p < 5 \times 10^{-10}$ ergs cm^{-2} s^{-1}), filled circles first bursts in double bursts, and open circles second bursts in double bursts.

temperature, dependent on the strength of the persistent emission and for a temperature of 1.6 keV increases from 4.4 ± 0.5 km to 8.7 ± 0.5 km as the persistent luminosity increases by a factor of 5.

3. The burst rate decreases as the persistent lumnosity increases. This decrease in burst rate is characterized by the appearance of irregular burst patterns at higher persistent flux levels where a sequence of bursts with intervals of ~ 3 hr is punctuated by a longer gap of > 5 hr. At lower persistent flux levels the burst intervals were only 2–3 hr.

4. Four bursts were detected that occurred within 10–20 minutes of a previous burst and had an α less than 10. These occurred only when the persistent luminosity was less than 6×10^{36} ergs s^{-1}. When the persistent luminosity was below this value, the double bursts were quite frequent with an occurrence rate of 0.16 per hour. The blackbody radius derived during the decay of each component of a double burst was identical for both and was also the same as that found during other bursts recorded at the same level. The total energy in the first burst in a pair was the same as in single bursts seen at the same persistent flux level while that in the second burst was only $\sim 30\%$ of this value.

The correlation of the burst properties of EXO 0748$-$676 with the strength of the persistent emission represents one of the best examples of such a dependence found to date. The burst sources MXB 1659$-$29 (Lewin *et al.* 1978; Lewin 1978) also showed a higher burst frequency at lower persistent flux levels, similar to the trend that we have observed from EXO 0748$-$676. In 4U 1820$-$30 (Clark *et al.* 1977) the burst recurrence time decreased while the persistent flux increased, but at a still higher persistent emission no bursts were seen. The burst frequency of XB 1608$-$52 remained constant when the persistent flux decreased by a factor of 7 (Murakami *et al.* 1980*a*). However, this decrease in flux was associated with a decrease in α from ~ 500 to less than 70 and a change in the burst profile from "fast" to "slow." Both of these trends are similar to the trend seen from EXO 0748$-$676. In addition the peak flux versus total flux diagram for the bursts from XB 1608$-$52 displayed the same bimodal distribution seen in Figure 9.

Most calculations of X-ray bursts assume that hydrogen is burned continuously via the CNO cycle because it becomes thermally unstable only at relatively low temperatures ($< 7 \times 10^7$ K, e.g. Ayasli and Joss 1982). Because the hydrogen will not be completely burned for accretion rates above $\sim 3 \times 10^{16}$ g s^{-1}, its additional contribution to the flash will tend to decrease α. Since the amount of available hydrogen will increase with mass accretion rate, α should correspondingly decrease. At high accretion rates approaching $\sim 10^{18}$ g s^{-1} the heating due to gravitational compression will dominate over any heating from continuous hydrogen burning. This should at some point lead to a reversal in the α/accretion rate relation such that α then increases with increasing accretion rate and at the highest accretion rates cause the helium burning to become stable, i.e., α becomes infinite. The range of luminosity seen from EXO 0748$-$676 of 0.4–2.2 $\times 10^{37}$ ergs s^{-1} is equivalent to mass accretion rates of 0.4–2.2 $\times 10^{17}$ g s^{-1} if 10% of the rest mass energy is converted into X-ray emission.

The correlation of α with accretion rate found for EXO 0748$-$676 is contrary to that expected from thermonuclear flash models that assume hydrogen is continuously burned. The α values of 20–30 obtained at the lowest accretion rates strongly suggest that hydrogen must provide a major source of fuel for the burst. This is qualitatively consistent with the interpretation of the XB 1608$-$52 observation (Murakami *et al.* 1980*a*) by Fujimoto, Hanawa, and Miyaji (1981) that at accretion rates below a critical value hydrogen burning turns off because there is insufficient replenishment to sustain the burning. The ensuing slow hydrogen flash may then heat the envelope sufficiently to trigger a helium flash. The change in the duration of the burst from fast to slow as the persistent flux decreased is also consistent with the view that hydrogen becomes a major constituent in the flash at low accretion rates. The numerical calculations show that helium flashes tend to be much faster than combined helium/hydrogen events (Taam 1980; Fujimoto, Hanawa, and Miyaji 1981).

A dependence between the color temperature and the apparent radius is to be expected because the peak of the blackbody spectrum will be distorted towards higher energies by free-free and bound-free transitions and Comptonization in the atmosphere of the neutron star (London, Taam, and Howard 1984; Ebisuzaki and Nomoto 1985). The ratio between the color (observed) temperature T_c and effective temperature $T_{\rm eff}$ is an increasing function of $T_{\rm eff}$ such that the apparent radius $R_a \approx f_x^{0.5}/T_c^2$ will be systematically underestimated for large T_c. This will cause R_a to be anticorrelated with T_c as the burst cools (Matsuoka 1985; Sztajno *et al.* 1985). This effect is seen in the fast bursts but is absent in the slow bursts where the radius remains constant despite a factor of almost 2 change in T_c.

The correlation of R_a with the strength of the persistent emission is surprising. The decrease in R_a at lower accretion rates might indicate that the area of the neutron star involved in the flash is a factor of 2 less (nonspherical burning), which also could support the view that the double bursts with low α (which are also only seen at low accretion rates) are caused by flashes from different parts of the neutron star. However, all the calculations made to date indicate that the whole neutron star surface will be involved in the flash. It also seems unlikely that the area of the two regions would be identical. In addition we would still expect the anticorrelation between R_a and T_c to be preserved irrespective of the area of the neutron star involved in the flash.

Because the distortion of the blackbody spectrum by the neutron star atmosphere is dependent on the chemical composition of the atmosphere (cf. London, Taam, and Howard 1984; Ebisuzaki and Nomoto 1985), a more promising explanation is that the structure and composition of the outer layers and/or the atmosphere of the neutron star changes with mass accretion rate. Any change in the accretion rate will therefore change the dependence of R_a on T_c. According to Ebisuzaki and Nomoto (1985) the difference in abundances can lead to different tracks in a T_c/L_a diagram, very similar to that seen for EXO 0748 − 676 in Figure 7. Variations in R_a for a given T_c already have been reported by Matsuoka (1985) for several different bursts seen from XB 1608 − 52. Although in this case no attempt was made to correlate these effects with the level of the persistent emission or α, it was also suggested that a different chemical composition in the burst atmosphere causes this effect.

The observed peak burst luminosities were 3.9×10^{38} ergs s^{-1} for the assumed distance of 10 kpc. These were seen only during the three bursts that displayed radius expansion. Since we have, as yet, no independent means of obtaining the distance to this source, we cannot comment on whether these bursts truly exceed the Eddington limit. When the bursts were slow (at lower persistent flux levels), the peak luminosities were $\leq 1 \times 10^{38}$ ergs s^{-1}, with in no case any evidence for radius expansion. If only those bursts where the radius remained constant are considered, the fast bursts tended to have peak burst luminosities a factor of 2 larger than their slow counterparts; this is consistent with these bursts being near the Eddington limit for, respectively, helium and hydrogen.

The energy released during a burst following a long gap is not directly proportional to the amount of material accumulated in the interim. This suggests that nuclear energy is lost in this interval, presumably by continuous burning during part of the gap (Joss and Rappaport 1984 and references therein).

Our observations of EXO 0748 − 676 have added four more double bursts to increase the total number of these events seen to 10 (cf. Matsuoka 1985 and references therein). The double burst phenomenon from this source is coupled to the accretion rate and is only present at low persistent flux levels. This suggests that the conditions that lead to the occurrence of double bursts is connected with the low α and smaller radii seen at similar flux levels. We have assumed that the correlation of α and R_a with persistent luminosity is caused by the flashes changing from helium dominated to hydrogen-triggered hydrogen-helium flashes. Double bursts occur only during the latter events. It may well be that the double bursts are the result of some incomplete reaction network in this regime, which, so far as we are aware, has not been explored as fully as the helium triggered flash.

VII. CONCLUSIONS

We have analyzed 22 bursts from the transient X-ray source EXO 0748 − 676 and found that their properties are a strong function of the strength of the persistent emission. The ratio α is found to decrease from 60–300 to 20–30 as the persistent luminosity decreases by a factor of 5, contrary to the predictions of calculations for nuclear flashes where the hydrogen burning is considered stable. We suggest that the persistent flux dependent variations in burst properties from this source are caused by the flashes changing from helium-dominated at high accretion rates, to hydrogen-triggered helium-hydrogen flashes at low accretion rates. This confirms a scenario first outlined by Fujimoto, Hanawa, and Miyaji (1981). The apparent blackbody radius for a given color temperature measured during the decay of the burst is found to depend also on the strength of the persistent emission and to decrease as the mass accretion rate decreases. We suggest that this is caused by a change in the composition in the atmosphere of the neutron star resulting from changes in the nuclear reaction networks. Double bursts were seen on four occasions where the α of the second burst was < 10. These only occurred at low persistent luminosities, where they became quite frequent. These double bursts may be a feature of hydrogen triggered hydrogen/helium flashes.

We thank the *EXOSAT* observatory team for their support. M. G. thanks Walter Lewin, and N. E. W. thanks Ron Taam for useful discussions.

REFERENCES

Ayasli, S., and Joss, P. C. 1982, *Ap. J.*, **256**, 637.
Basinska, E. M., *et al.* 1984, *Ap. J.*, **281**, 337.
Clark, G. W., *et al.* 1977, *M.N.R.A.S.*, **179**, 651.
de Korte, P. A. J., *et al.* 1981, *Space Sci. Rev.*, **30**, 495.
Ebisuzaki, T., and Nomoto, K. 1985, in *Japan-US Seminar on Galactic and Extragalactic Compact X-Ray Sources*, ed. Y. Tanaka and W. H. G. Lewin (Tokyo: Institute of Space and Astronautical Science), p. 101.
Fujimoto, M. Y., Hanawa, T., and Miyaji, S. 1981, *Ap. J.*, **246**, 267.
Joss, P. C. 1977, *Nature*, **270**, 310.
Joss, P. C., and Rappaport, S. A. 1984, *Ann. Rev. Astr. Ap.*, **22**, 537.
Lewin, W. H. G. 1978, *IAU Circ.*, No. 3193.
Lewin, W. H. G., *et al.* 1976, *M.N.R.A.S.*, **177**, 83P.
——— 1978, *IAU Circ.*, No. 3190.
Lewin, W. H. G., van Paradijs, J., Cominsky, L., and Holzner, S. 1980, *M.N.R.A.S.*, **193**, 15.
London, R. A., Taam, R. E., and Howard, W. M. 1984, *Ap. J.* (*Letters*), **287**, L27.
Maraschi, L., and Cavalier, A. 1977, *Highlights Astr.*, **4**, 127.
Matsuoka, M. 1985, in *Japan-US Seminar on Galactic and Extragalactic Compact X-Ray Sources*, ed. Y. Tanaka and W. H. G. Lewin (Tokyo: Institute of Space and Astronautical Science), p. 45.
Murakami, T., *et. al.* 1980*a*, *Ap. J.* (*Letters*), **240**, L143.
———. 1980*b*, *Pub. Astr. Soc. Japan*, **32**, 543.
Ohashi, T., *et al.* 1982, *Ap. J.*, **258**, 254.
Parmar, A. N., White, N. E., Giommi, P., and Gottwald, M. 1986, *Ap. J.*, **308**, 199 (Paper I).
Parmer, A. N., White, N. E., Giommi, P., and Haberl, F. 1985, *IAU Circ.*, No. 4039.
Peacock, A., *et al.* 1981, *Space Sci. Rev.*, **30**, 525.
Sztajno, M., *et al.* 1985, *Ap. J.*, **299**, 487.

Taam, R. E. 1980, *Ap. J.*, **241**, 358.
———. 1981, *Ap. J.*, **247**, 257.
Taam, R. E., and Picklum, R. E. 1978, *Ap. J.*, **224**, 210.
———. 1979, *Ap. J.*, **233**, 327.
Turner, M. J. L., Smith, A., and Zimmermann, H. U. 1981, *Space Sci. Rev.*, **30**, 513.
Vacca, W. D., Lewin, W. H. G., and van Paradijs, J. 1985, *M.N.R.A.S.*, submitted.
Woosley, S. E., and Taam, R. E. 1976, *Nature*, **263**, 101.

Manfred Gottwald, Frank Haberl, Arvind N. Parmar, and Nick E. White: EXOSAT Observatory, ESOC, Robert-Bosch-Strasse 5, D-6100 Darmstadt, West Germany